

## **Development of Source Apportionment Algorithms**

### **12. Using mass spectral source signatures to apportion exhaust particles from gasoline and diesel powered vehicles in a freeway study using UF-ATOFMS**

#### **i. Introduction**

Many studies have shown that vehicle emissions represent a major source of pollution in urban areas (399-403). With growing concern over the health effects pertaining to pollution from vehicles (280,404,405), a goal of major federal and state agencies is to set regulations which will lead to a reduction of pollutants from these sources. The first step in this process involves distinguishing between the emissions from gasoline powered light duty vehicle (LDV), heavy duty diesel vehicle (HDDV), and other combustion sources in ambient aerosols which will allow state and federal air control agencies to quantify the relative contributions from the major pollution sources and develop effective control strategies.

Several methods have been used for aerosol source apportionment using a variety of techniques. Filter and impactor sampling methods, such as Micro Orifice Uniform Deposit Impactors (MOUDI), are useful in collecting particles that can be chemically analyzed using a variety of off-line techniques. These techniques have proved useful in determining organic markers for various aerosol sources in the atmosphere (170,406,407). On-line measurements are being used more and more for source apportionment. Some of these instruments include Scanning Mobility Particle Sizers (SMPS), where particle source contributions are estimated based on the measured size modes of the particles (408-410). Other on-line instruments, such as Thermal Desorption Particle Mass Spectrometers (TDPMS) and Aerosol Mass Spectrometers (AMS) have been used for particle source apportionment as well (411-413). However, these thermal desorption techniques are unable to detect refractory components (such as inorganic compounds and elemental carbon), and they do not sample single particles. Single particle techniques such as aerosol time-of-flight mass spectrometry (ATOFMS) provide an alternative method for source apportionment (87,414-416). The ATOFMS uses a laser to desorb and ionize species from individual particles and thus can detect all chemical species (refractory and non-refractory) of each particle simultaneously with a dual polarity time-of-flight mass spectrometer (127,417). An ultrafine aerosol time-of-flight mass spectrometer (UF-ATOFMS) was used in this study, because the majority of particles emitted in both LDV and HDDV exhaust are in the ultrafine size range (aerodynamic diameter ( $D_a$ ) < 100nm).

The purpose of this study involves determining whether mass spectral signatures obtained from previous vehicle dynamometer characterization studies are representative of those detected in an area with fresh roadside emissions (37,418,419). Logistically, a freeway-side location was chosen in a coastal “clean” environment so there would be little influence from sources other than vehicles. Also, in such a location, the particles would be less aged which would “skew” the mass spectral signatures. A major objective of this study is to test whether the ART-2a neural network clustering algorithm matching

method can be used to distinguish mass spectral signatures from very similar vehicle sources. Finally, upon method validation, the goal is to apportion aerosols near the roadway and determine their overall contribution to the total ambient aerosol at the freeway location.

## ii. Experimental

This study was conducted in San Diego, California from Jul. 21-Aug. 25, 2004. The sampling site was stationed in a low-use parking lot during the summer on the UCSD campus directly adjacent to the I-5 freeway (GPS position 32°52'49.74"N 117°13'40.95"W) with the sampling line within 10 meters of the freeway. The site housed a suite of instruments including an UF-ATOFMS. This same UF-ATOFMS instrument was used in two previous studies for the characterization of aerosols from LDVs and HDDVs (37,418). A summary of the instrumentation operated at the site (that will be discussed in this paper) is provided in **Table 15**. Meteorological stations were operated on each side of the freeway for complete wind trajectory information. A digital Webcam was used for freeway traffic monitoring and recorded digital video continuously throughout the study.

Traffic counts were determined by counting individual LDVs and HDDVs on both sides of the freeway for the first five minutes of each hour. The number of vehicles counted in the first five minutes was multiplied by twelve in order to approximate the total LDV and HDDV counts for the entire hour. The LDV fleet consisted primarily of newer vehicles (model year 2000 or newer), which was determined by routine traffic observations and from the video. The HDDV fleet along this portion of the freeway was predominantly tractor trailers, with a much smaller contribution from buses and medium sized diesel delivery trucks.

Instrument	Make & Model	Measurement	Units	Sample Resolution	Sampling Period
Ultrafine Aerosol Time-of-Flight Mass Spectrometer (UF-ATOFMS)		size range: 50-300nm		real-time	Jul 21 to Aug 25, 2004
Scanning Mobility Particle Sizer (SMPS)	TSI Model 3936L10	particle number conc. (10-500nm)	#/cm <sup>3</sup>	5 min	Jul 21 to Aug 25, 2004
Aethalometer	Magee Scientific 'Spectrum' AE-3 Series	optical absorption cross-section per unit mass	µg/m <sup>3</sup>	5 min	Jul 21 to Aug 25, 2004
Chemiluminescence NO-NO <sub>2</sub> -NO <sub>x</sub> Analyzer	Thermo Environmental Instruments (TEI) Model 42C	NO & NO <sub>x</sub> concentration levels	ppb	1 min	Aug 5 to Aug 25, 2004
CO Analyzer	Advanced Pollution Instrumentation (API) Model M300	CO concentration levels	ppm	5 min	Jul 30 to Aug 10 & Aug 13 to Aug 25, 2004
Webcam	Creative Model PD1001	traffic video surveillance		1 sec	Jul 21 to Aug 25, 2004

Table 15: List of instrumentation.

The particle mass spectra from the vehicles studies were previously analyzed and clustered with the ART-2a clustering algorithm as described in Sodeman *et al* and Toner *et al* (37,418). The ART-2a algorithm and its use for single particle characterization are described in detail elsewhere (10,420). ART-2a has been compared to other approaches (8) where it is shown that ART-2a yielded very comparable results to other clustering techniques including several variants of hierarchical clustering as well as K-means clustering. For the PM emissions in vehicle studies, the ART-2a parameters used were a vigilance factor (VF) of 0.85, learning rate of 0.05, and 20 iterations. The resulting mass spectral signatures (clusters) were used to apportion particles detected near the freeway using the same ART-2a algorithm, but using a matching approach. The match-ART-2a function (YAADA v1.20 – <http://www.yaada.org>) uses existing ART-2a clusters as source “seeds” for the purpose of determining whether other particles match those seeds. In this case, ART-2a runs normal with prescribed particle clusters unable to be changed by the addition of new particles to each cluster. Since the clusters do not change as particles are matched to them, this function allows the clusters to stay “true” to the original source signature. Particles being considered in the matching are either matched exclusively to a particular cluster (above the VF) or not at all. If a particle matches above the threshold for two or more clusters, it will be added to the one with which yields the highest dot product. The VF used for match-ART-2a for this study is 0.85 which represents a very high VF. If the dynamometer signatures are truly representative of the signatures from vehicles, this VF should be effective because the vehicle emissions are expected to be fresh near the freeway. In a more aged environment, it is likely a lower VF will be necessary to match a reasonable number of particles. The effect of varying VF for source matching is discussed in Appendix 2.

The results obtained from match-ART-2a were compared to various peripheral data, to validate the results of the matching technique. Such peripheral instruments are described in **Table 15**. The outcome of these comparisons will be discussed below.

### iii. Results and Discussion

#### *a. Creation and Comparison of Particle Seeds From Source Studies*

As described in the Experimental section, the particles detected with the UF-ATOFMS during the freeway-side study were analyzed via a matching version of the ART-2a algorithm. The particle clusters used for matching (as the reference library) were obtained in previous LDV and HDDV dynamometer studies (37,418,419). While the papers written on these studies refer to distinct particle classes, these classes are descriptive of the many (~100) ART-2a clusters resulting from the studies. Since ART-2a does not converge, these classes were grouped by running ART-2a and then regrouped using a function that combines resulting ART-2a clusters that match above a set vigilance factor (regrouped VF = 0.90). These regrouped clusters can then be even further grouped based on visual inspection of the ion patterns. Similar clusters that appear to belong within the same “class” as each other based on the presence or absence of key species (i.e. elemental carbon (EC), organic carbon (OC), sulfate, nitrate) are regrouped by hand. Such classes have minor differences in the relative ion peak patterns among their collective clusters, however; the overall chemical species making up each major type of cluster are the same.

For matching purposes, instead of using the combined weight matrices from the regrouped representative particle classes, the top ART-2a clusters that account for ~90% of the particles from each vehicle study were used. Additionally, it was hypothesized that the top particle types detected in the vehicle studies should also be the top types detected in the fresh emissions near the highway. In order to create source seeds more representative of the freeway environment, only particles generated during warm/hot engine conditions for both HDDV and LDV studies were used to make the source seed clusters. These clusters still correspond to their representative classes described in previous papers (as stated earlier), however, there are minor differences in some clusters that make it more advantageous to use the separate ART-2a clusters for matching purposes. In addition, clusters generated by running ART-2a on the UF-ATOFMS freeway detected particles were also incorporated into the source seed library. The majority of these clusters were attributed to HDDVs, as their weight matrices correlated much better to the HDDV library source seeds than to the LDV seeds. The seeds are also separated by size, where ultrafine (50–100nm) and accumulation mode (100–140nm & 140–1000nm) mass spectral libraries have been created for each source. This is done because there are distinct chemical differences for each source based on size, and these size ranges show the largest chemical distinctions. For example, as found in the dynamometer studies using UF-ATOFMS, LDVs produce more organic carbon than elemental carbon particles for sizes above 100 nm. Two separate libraries were made for the accumulation mode to compensate for a regional background elemental carbon particle type that was detected above 140nm during the freeway study. This particle type will be discussed in a future publication (421). For this manuscript, the matching results obtained from both accumulation mode libraries are combined to represent the UF-ATOFMS accumulation mode results (100–300nm). This was done because the trends in HDDV/LDV apportionment were found to be very similar between the two accumulation mode libraries once the regional background EC particles above 140 nm were identified as non-freeway particles. Further details on the number of seeds in the vehicle source library and the frequency at which they match particles for this study are provided in Appendix 1.

Since HDDVs and LDVs combust chemically similar fuels, it is important to first investigate the similarity between the HDDV and LDV exhaust particle types from the dynamometer source studies. The first method used to compare these particle types involved taking the representative area matrix for each class described for each study and calculating the dot product between them. The area matrices used to represent the particle classes are similar to the weight matrices that ART-2a yields except that the area matrices are not weighted. The area matrices represent an average of all particles within a particular class. Since ART-2a distinguishes particle types bases on their dot products, this type of comparison between the two studies allows one to determine if the area matrices of the general particle types would be distinguishable using ART-2a. **Figure 86** displays a color mapped table of this comparison, with cooler colors (i.e. blue) indicating less similarity (lower dot product) and warmer colors (i.e. red) indicating more similarity (higher dot product). The labels for the classes are based on the most abundant ion peaks in the mass spectra and are described in detail in previous source characterization manuscripts by Sodeman et al. and Toner et al. (37,418). **Figure 86** shows that some of the dot product comparisons between the two

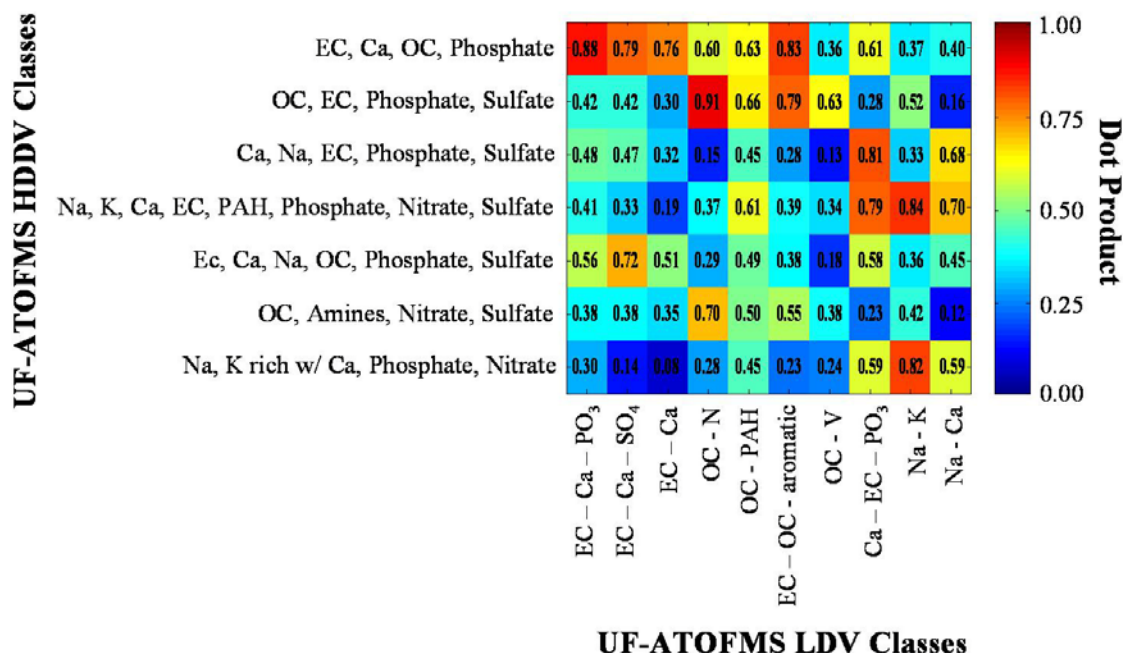


Figure 86: Dot product comparisons of the representative area matrices between the general classes from the HDDV and LDV dynamometer experiments using UF-ATOFMS. Classes are labeled in the same manner as in the manuscripts from Sodeman *et al.* 2005 and Toner *et al.* 2006.

source studies result in strong matches (i.e. orange and red colors). As expected, those classes that match the best are chemically similar types; i.e. the EC, Ca, OC, Phosphate classes from HDDV matching to the EC-Ca-PO<sub>3</sub> class from LDV (note this was produced by a smoking LDV). Also, the OC, EC, Phosphate, and Sulfate classes from HDDV match to the OC-N class from LDV. While these classes have dot products above the vigilance factor used for ART-2a analysis (VF = 0.85), they are visually distinct (as described in the two manuscripts) and still readily distinguishable using the matching procedure. One of the major problems with this comparison is the fact that the area matrices represent an average of the particles within the class and are not weighted to the majority. As stated previously though, the representative spectra of the general classes are not used for apportionment matching purposes. Instead, the size segregated mass spectral libraries for HDDV and LDV particles, as described above, are used. Using size information in the apportionment turns out to be quite important because those particles that are chemically similar between sources fall into quite different size ranges.

Another method for comparing the two studies involves taking the particles from the dynamometer studies detected with the UF-ATOFMS and matching them to the HDDV/LDV reference library clusters using a non-exclusive matching process with ART-2a. This process adds a matched particle to HDDV, LDV, or combination of both cluster types if the particle matches above a vigilance factor of 0.85. This method of matching allows for determining the amount of similarity of the particle types between the two studies. Between 19 – 33% of the HDDV dynamometer particles and 30 – 49% of the LDV dynamometer particles matched both the HDDV and LDV reference clusters. These results are shown in **Figure 87**. With such a large degree of overlap between the

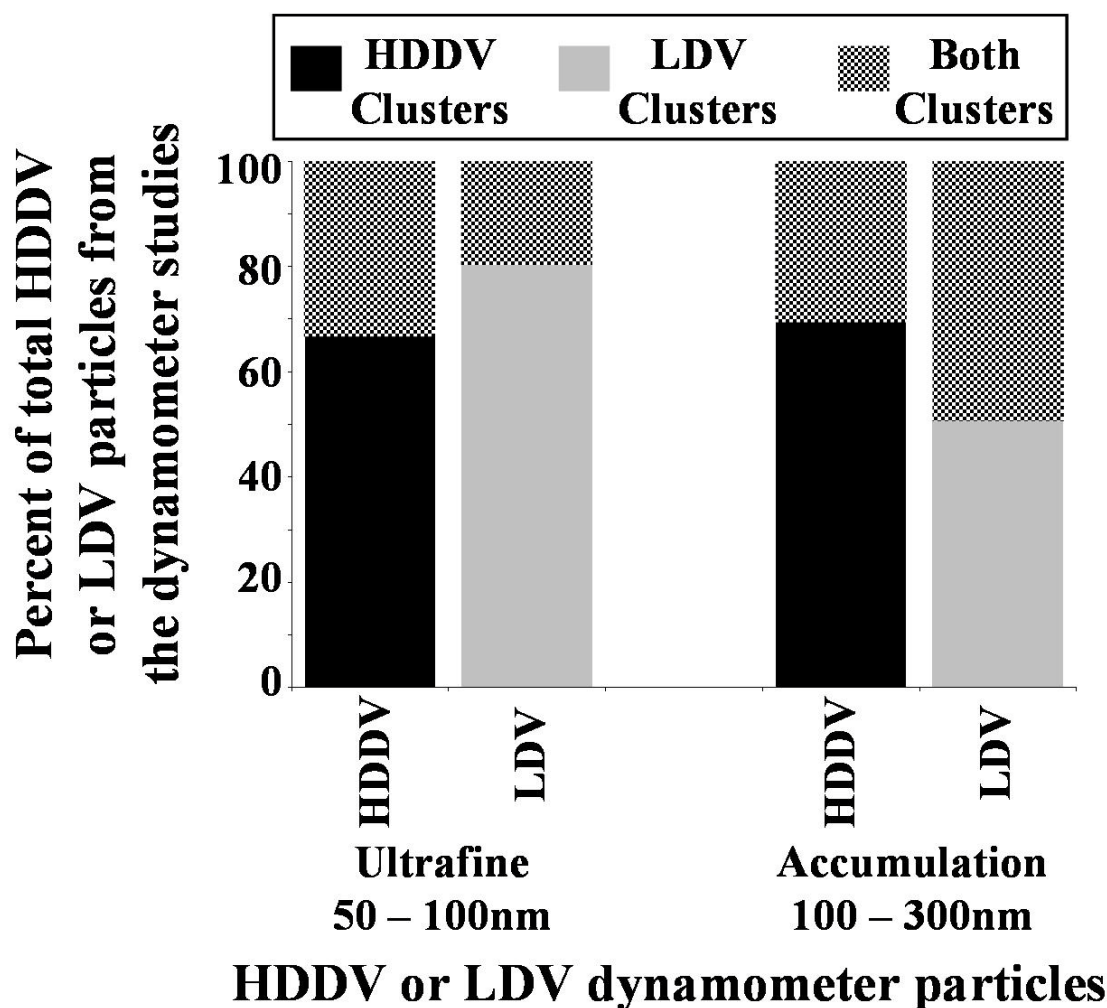


Figure 87: ART-2a matching error analysis using non-exclusive matching of HDDV and LDV dynamometer particles. For each, the fraction of HDDV and LDV particles that matched to the HDDV, LDV, or both HDDV and LDV clusters from the HDDV/LDV reference library are shown for ultrafine (50–100nm) and accumulation (100–300nm) mode particles.

particle types from both clusters, it would appear to be a challenging task to distinguish between HDDV and LDV particles using the ART-2a matching method. This is not the case though as particles within the overlapping region turn out to be quite distinguishable for reasons described below.

The main goal of this paper involves using ART-2a to distinguish between HDDV and LDV particles in an environment dominated by relatively fresh vehicle emissions. To accomplish this, an exclusive matching procedure was used where particles were matched to the HDDV/LDV reference clusters and they either matched exclusively or not at all. If a particle matched to more than one cluster above the vigilance factor, it was placed in the cluster to which it matched the most closely (i.e. the highest dot-product value). If a particle did not match to either HDDV or LDV, it was placed into the “other” category. Particles falling into the “other” category included sea salt, dust, biomass burning, and other sources not related to LDV or HDDV exhaust emissions. Quality assurance of this matching technique was carried out by using the same HDDV/LDV

cluster library to match to particles from the previous source studies. The amount of error in matching was calculated based on the number of particles from the known source that matched to the incorrect source. **Figure 88** shows the matching fraction of particles from each study to the same HDDV/LDV reference library. The most error (mismatching) is about 4%, which occurs for the larger accumulation mode particles from the LDV source particles matching to HDDV clusters within the reference library. Given this low error, this provides confidence in the ART-2a apportionment approach used in this study. The errors associated with matching to the source seeds at varying VF's, as well as results from using source seeds created at a lower VF, are discussed in Appendix 2.

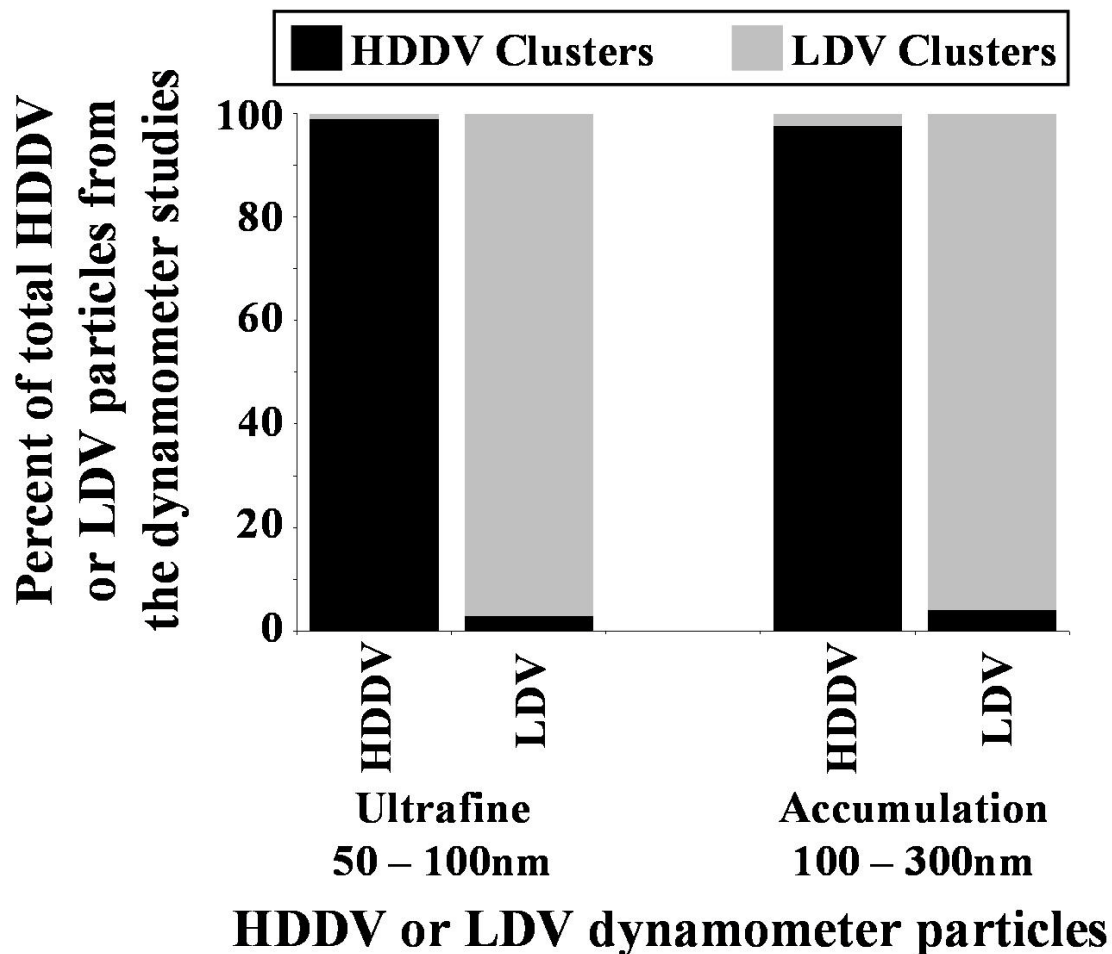


Figure 88: ART-2a matching error analysis using exclusive matching of HDDV and LDV dynamometer particles. For each, the fraction of HDDV and LDV particles that matched to the HDDV or LDV clusters from the HDDV/LDV reference library are shown for ultrafine (50–100nm) and accumulation (100–300nm) mode particles.

#### ***b. Particles Detected that Match to HDDV/LDV Source Seeds***

The ART-2a algorithm was used to cluster the particles detected with the UF-ATOFMS during the freeway-side study using a VF of 0.85. This approach creates the top particle types separately from the match-ART-2a technique to determine how closely the

resulting clusters compare with those from the vehicle studies. **Figure 89** (A-D) shows the representative ART-2a weight matrices (WM) /spectra from this analysis that match to the top particle types from the dynamometer studies. The top particle classes from the HDDV and LDV vehicle source characterization studies were used for this comparison because they should theoretically be the top particle types seen in a vehicle dominated environment. Indeed, this is the case, where the majority of the top ten freeway ART-2a results match to the top HDDV dynamometer classes. The top HDDV particle type detected from the dynamometer studies is the top type detected during this freeway-side study (as shown in **Figure 89A**) and matches with an  $R^2$  of 0.97 when the  $m/z$  peak pattern and intensities are plotted against each other. **Figure 89B** shows the second most abundant type from the HDDV dynamometer studies compared to the second most abundant type detected during the freeway study which matches with an  $R^2$  of 0.98. This particle class is also the most abundant type detected in 100 – 400 nm particles detected with a standard inlet ATOFMS (419). The spectra shown in **Figure 89C** represent the third cluster from the freeway ART-2a results which match the top LDV type from the dynamometer study with an  $R^2$  of 0.99. The last



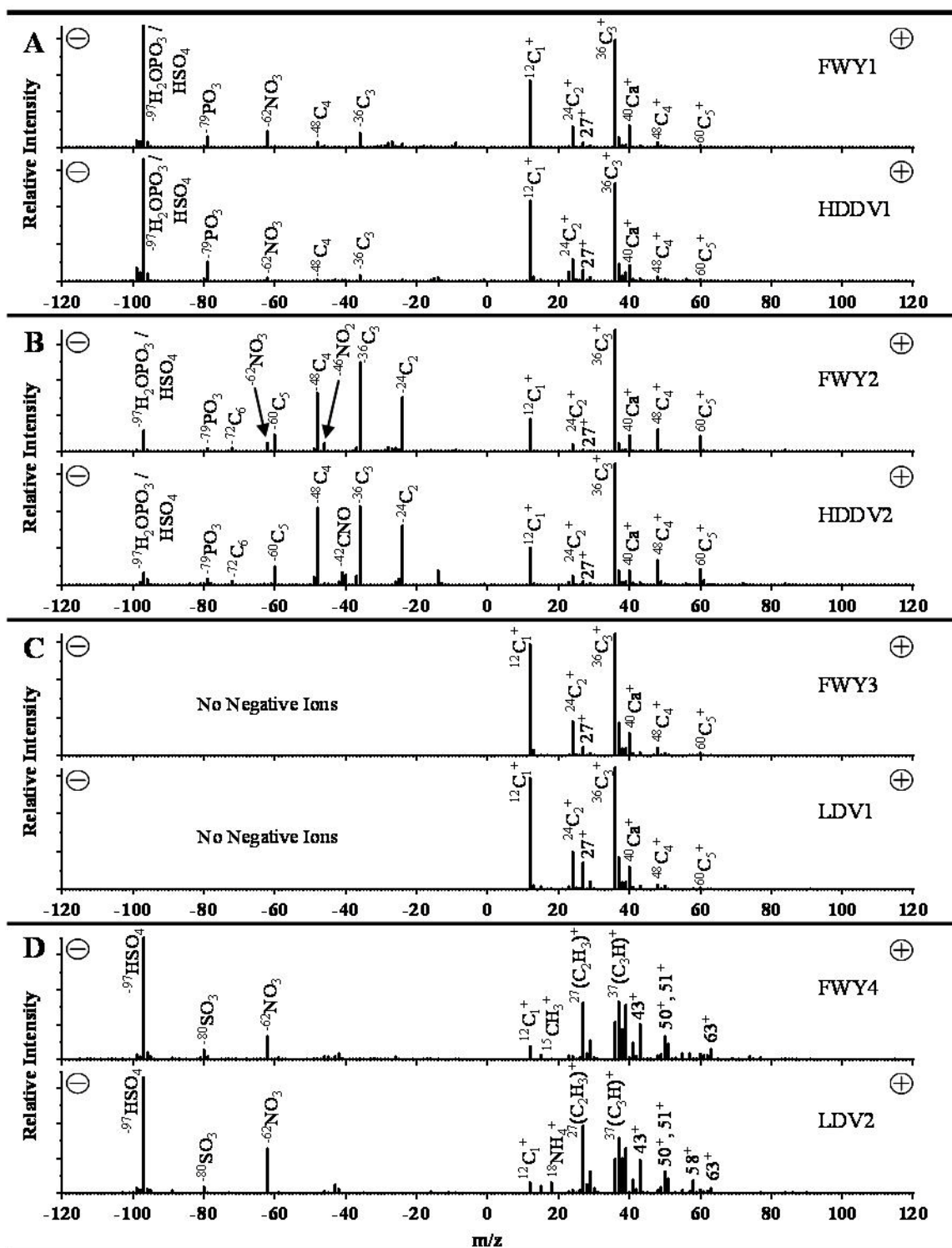


Figure 89: Weight matrices of the top particle types detected during freeway study that match to vehicle study signatures.

spectra (**Figure 89D**) show the sixth freeway particle cluster that matches the third most abundant type from the LDV dynamometer study ( $R^2 = 0.98$ ).

There has been speculation as to whether mass spectral signatures from different sources obtained from laboratory and dynamometer experiments can be detected during ambient studies and used for source apportionment purposes. Such questions result from the concern that the dilution and residence systems used during source characterization studies do not properly mimic real-world dilution and aging conditions that occur in on-road driving exhaust (422,423). The freeway-side study was chosen to lessen the effects of aging on the particle signatures. It was expected that the “fresh” emissions would be more comparable to the particle signatures obtained from the dynamometer experiments. The high  $R^2$  values for the comparison of particle classes confirms the chemistry of the particle types detected in dynamometer studies are consistent with those produced in ambient environments.

The high  $R^2$  values serves as further validation that the ART-2a clustering technique is a reliable method for ATOFMS particle mass spectral clustering. A discussion of whether mathematical clustering algorithms can properly separate and cluster similar particle types has been addressed in the literature (6,414,424). Some concerns about ART-2a have included that too low of a vigilance factor will yield a manageable number of end clusters, but will not distinguish between different types of particles. Also, too high of a vigilance factor will yield too many clusters to properly classify all particles. Through laboratory work conducted with ATOFMS data of known particle types, the proper vigilance factor for source apportionment using ART-2a has been found to be 0.85 (245). While this tends to create many clusters for ambient data sets, the number is quite manageable because similar clusters can still be mathematically regrouped (which greatly reduces the number of clusters). For example, in this freeway study 2,763 clusters were generated after running ART-2a ( $VF = 0.85$ ) on fine mode particles, but mathematically regrouping these clusters using a  $VF$  of 0.90 reduces the number to 370 clusters (of which, the top 72 represent 90% of the total freeway-side particles detected with the UF-ATOFMS). The  $R^2$  values obtained for these comparisons show that these techniques work very well and should lessen concerns about their legitimacy.

### *c. Temporal Trends and Correlations with UF-ATOFMS Data*

A number of peripheral instruments accompanied the UF-ATOFMS instrument for this study to test the apportionment process being used. Previous vehicle apportionment studies show that  $NO_x$  emissions can be used as a tracer gas for HDDV emissions (425-427). Also, an aethalometer measures absorptivity by particles and can be used as an indicator of elemental carbon (or soot) containing particles (particularly at  $\lambda = 880\text{nm}$ ). Indeed, previous HDDV and LDV source studies show more EC associated with HDDVs (37,418,419). CO gas emissions have been shown to act as a tracer for LDV emissions (426); however, the CO monitor used in this study was not running during all the time periods. **Figure 90** (A,B) shows a plot of  $NO_x$  vs. aethalometer data as well as HDDV counts (from video footage) vs. aethalometer. The time periods for the two plots are different as the  $NO_x$  monitor began later in the study. However, the plot between the  $NO_x$  and aethalometer (**Figure 90A**) show a good

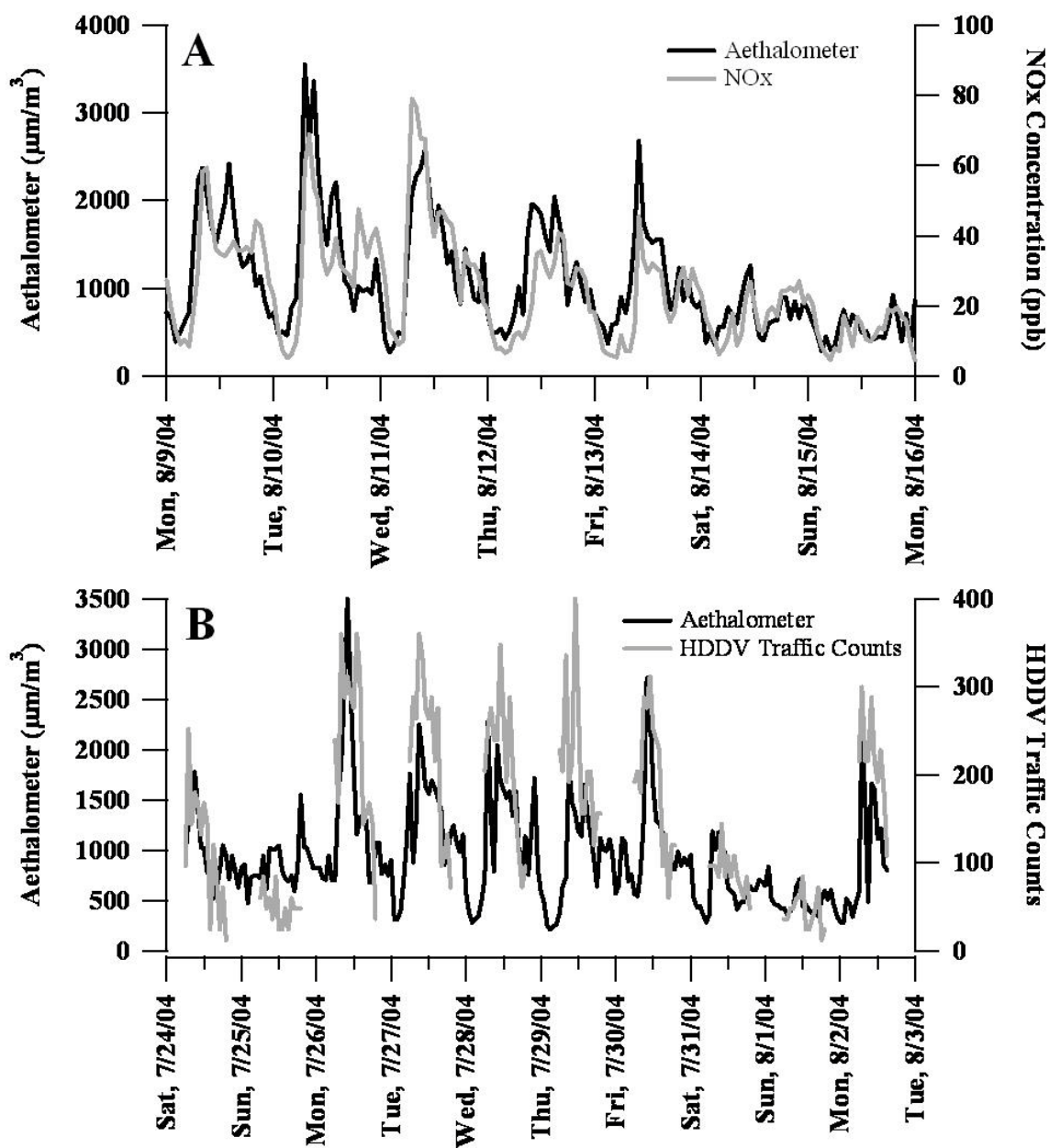


Figure 90: Temporal plots of A) NO<sub>x</sub> gas data vs. aethalometer data; and B) HDDV video counts vs. aethalometer data. Both NO<sub>x</sub> and aethalometer data show a good correlation with each other ( $R^2 = 0.7$ ). The HDDV video counts also track the aethalometer data.

correlation ( $R^2 = 0.7$ ), tracking for the remainder of the study, which suggests it is safe to assume that they most likely tracked during the time period before the NO<sub>x</sub> instruments arrival. This correlation can allow the use of the aethalometer data trends as a surrogate for the NO<sub>x</sub> concentrations during periods when the NO<sub>x</sub> data were not available. **Figure 90B** shows the comparison of HDDV video counts versus the aethalometer trends. The breaks in the counts come at night when there is insufficient light to properly distinguish

between vehicles. The trends in HDDV counts versus aethalometer data also show a very strong correlation. Since HDDV's are shown to emit a larger mass of black carbon compared to LDV's (428,429), it is expected that the HDDV counts should be closely correlated with the aethalometer data. HDDVs make up about 2% of the fleet for this particular region of the freeway, and when HDDV traffic counts peak, there is generally a very large amount of LDV traffic as well. Even though HDDVs make such a low contribution to the traffic on this stretch of freeway, their particle emissions are quite prevalent and readily discernable.

**Figure 91** and **Figure 92** shows the time series of the ART-2a matching results for the fine and ultrafine mode particles, respectively. Using the fractions from both the ultrafine and fine mode temporal plots, on average 83% of the aerosols detected near this roadside with the UF-ATOFMS are attributed to vehicle exhaust emissions, with 32% apportioned to LDV and 51% to HDDV emissions. For the fine mode particles ( $D_a = 100\text{--}300\text{nm}$ ), 66% of the aerosols are attributed to vehicle exhaust emissions, with 25% from LDV and 41% from HDDV. And, for ultrafine particles ( $D_a = 50\text{--}100\text{nm}$ ), 95% of the aerosols are apportioned to vehicles, with 37% from LDV and 58% from HDDV. The fact that such a large number of particles in the roadside environment matched to the vehicle seeds using a relatively high vigilance factor (0.85) produces confidence that the seeds used in the source library are representative of a broad range of vehicles. If a particular particle type had been missed in the seeds, it would be apparent in a large number of "other" particles.

**Figure 91** shows the ART-2a matching results for fine mode particles ( $D_a = 100\text{--}300\text{nm}$ ) along with wind data and video traffic counts for July 24 to Aug 03, 2004. This time period is of particular interest because MOUDI samplers ran at the same time and the source apportionment results from both approaches will be compared in a future study. The plot of the unscaled matching counts shows that both wind and traffic counts play a major role in the particle concentrations for this site. The matching counts peak around 9:00 each morning, which is when HDDV traffic counts peak. This also occurs just prior to, and during the beginning of daily peak wind speeds. The sampling site was located on the east side of the freeway because the prevailing daily wind blows from the west ( $270^\circ$ ). This allowed for the ideal positioning to detect freeway traffic exhaust particles. The matched fraction and unscaled count plots show that there is a larger number of diesel particles detected (relative to LDV matched particles), which follow the trend in diesel traffic observed from the video footage. It is interesting to note that the detection of LDV particles is always lower than that of HDDV particles for the fine particle mode. This was expected, as roadside and ambient studies have shown that HDDV's contribute a much higher concentration of particles even in LDV dominated areas (410,430-432). Vehicle studies have also shown that HDDV's emit a significantly higher fraction

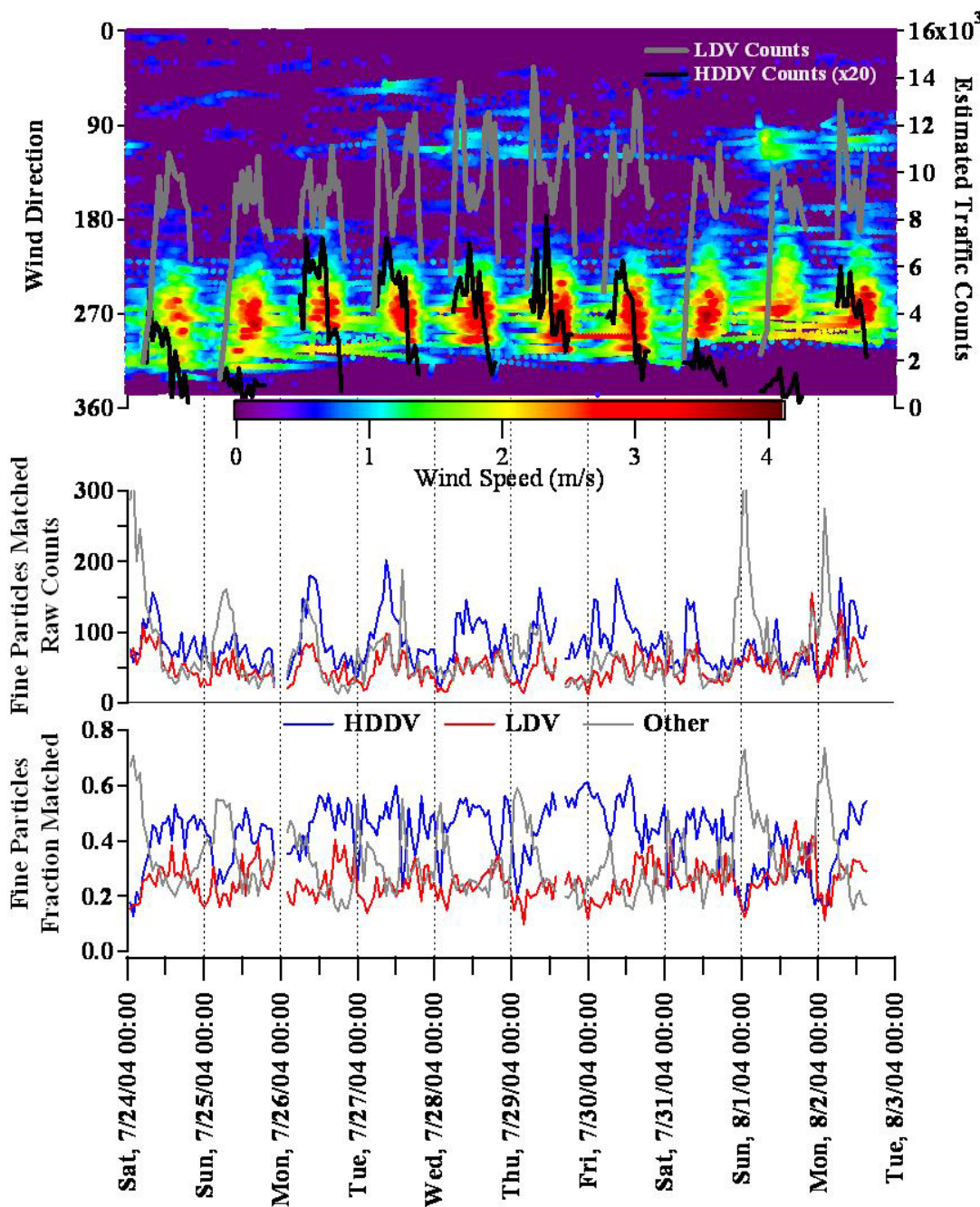


Figure 91: Top: Wind data (blowing from: N = 0°/360°, E = 90°, S = 180°, W = 270°) along with LDV & HDDV traffic counts (from video). HDDV counts are multiplied by 20 to keep them on the same scale as LDV traffic counts. Middle: HDDV/LDV/Other ART-2a matching result unscaled counts from UF-ATOFMS data. Bottom: HDDV/LDV/Other ART-2a matching fraction results from UF-ATOFMS data. Data shown are accumulation mode particles ( $D_a = 100\text{--}300\text{nm}$ ) for July 24 to Aug 03, 2004.

of fine particles compared to LDV's (37,418,419). Another note to make about **Figure 91** is that the temporal trend for the fraction of particles attributed to other sources has no

correlation with the fractions matched to HDDV or LDV. This randomness of the accumulation mode “Other” type indicates that the particles within this class are not associated with either fresh HDDV or LDV emissions.

**Figure 92** shows the times series of the ART-2a matching results for ultrafine particles ( $D_a = 50\text{--}100\text{nm}$ ) along with SMPS data and video traffic counts for July 24 to Aug 03, 2004. Traffic counts are shown on both **Figure 91** and **Figure 92** to allow for comparison. This figure depicts how strong of a role the traffic counts play on the particle concentrations detected at this site. Comparing the ultrafine unscaled matched counts to the SMPS data illustrates how well the UF-ATOFMS particle detection tracks the changes in particle concentrations at this site. Since ultrafine particles provide an indication of freshly emitted particles, it was expected that the UF-ATOFMS ultrafine counts would track the SMPS data and the vehicle counts. This figure also shows how strong an influence the LDV emissions, though still less than HDDV emissions, have on the ultrafine particle concentrations in this area versus the fine mode particles. The fraction plot shows that there is a fairly consistent trend between the LDV and HDDV contribution to the ultrafine mode. As was discussed for **Figure 91** in reference to the fine particles, HDDV's are known to emit a greater number of ultrafine particles in comparison to LDV's (37,418,419). Once again, this can account for the larger number of HDDV particles detected by the UF-ATOFMS than for LDV's, despite the dominating LDV traffic counts. Another note



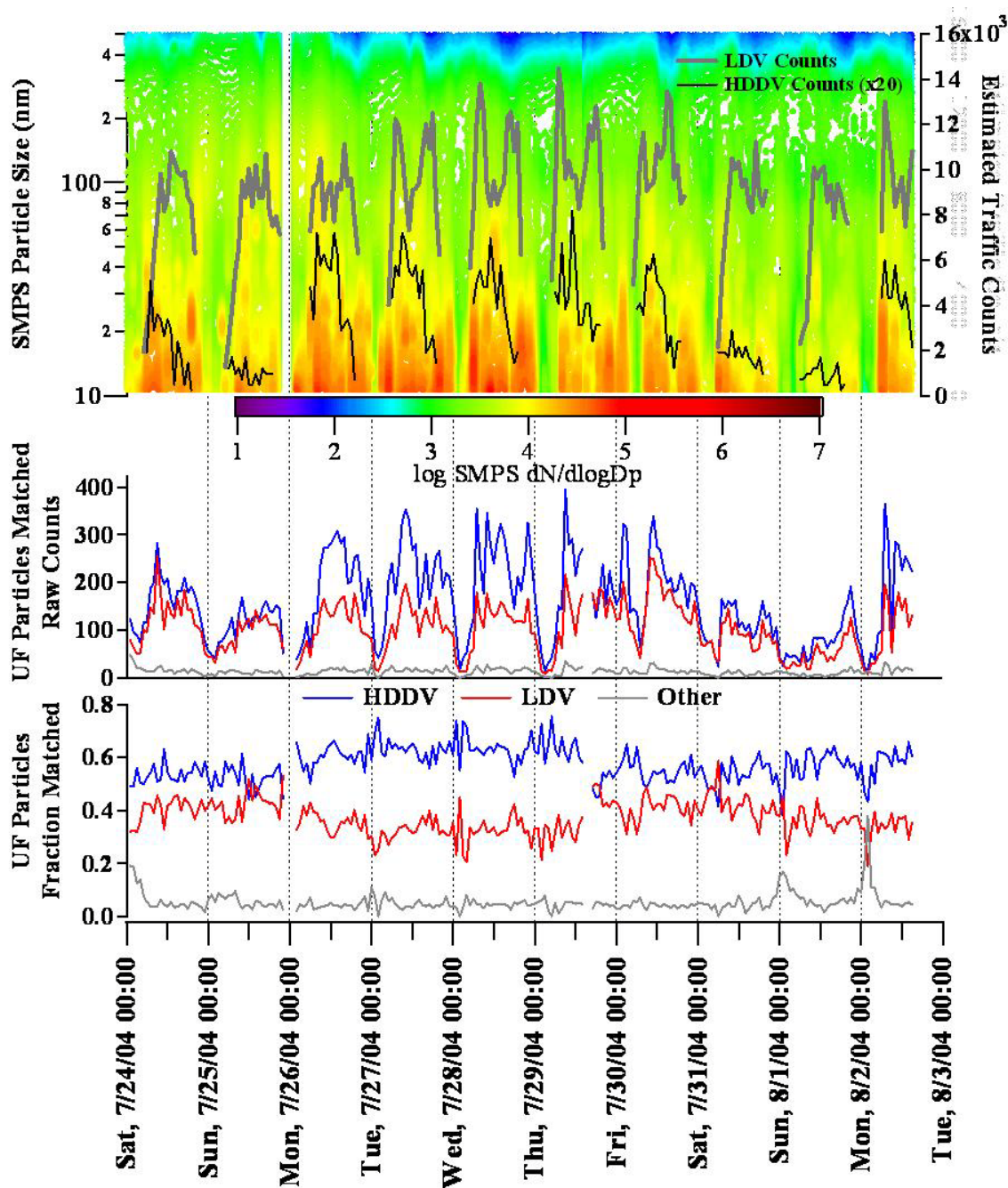


Figure 92: Top: SMPS data along with LDV & HDDV traffic counts (from video). HDDV counts are multiplied by 20 to keep them on the same scale as LDV traffic counts. Middle: HDDV/LDV/Other ART-2a matching result unscaled counts from UF-ATOFMS data. Bottom: HDDV/LDV/Other ART-2a matching fraction results from UF-ATOFMS data. Data shown are ultrafine mode particles ( $D_a = 50\text{--}100\text{nm}$ ) for July 24 to Aug 03, 2004.

to make about **Figure 92** is that it clearly shows a difference in weekday versus weekend traffic and particle detection. The first Saturday (7/24/04) had a high amount of traffic,

including HDDV traffic, and shows almost the same amount of matching contributions as the weekdays. The first Sunday (7/25/04), as well as the following weekend show a reduced amount of HDDV traffic and, hence, a lower number of particles matching to HDDVs. When HDDV traffic increased on the weekdays, the number of HDDV apportioned particles were much greater than those apportioned to LDV's. It wasn't until Friday (7/30/04) that the LDV detected UF particle counts began to resemble those for HDDV's, and they remained about even through the weekend. Then, on Monday (8/02/04), the HDDV emissions began to dominate again. Also, an interesting feature to note about **Figure 91** & **Figure 92** is that while the weekend LDV video counts remained relatively high (especially compared to the HDDV counts), the fraction of LDV and HDDV particles did not seem to change by the same magnitude. The weekend HDDV fraction goes down by about 10% for the UF particles and 9% for the accumulation mode particles, while the LDV fraction goes up by 7% for the UF particles and 2% for the accumulation mode. Also, the LDV apportioned counts go down despite the video traffic counts staying relatively high due to the fact that the winds were not as strong towards the site on the weekend as they were throughout the week. On 8/1, in addition to the winds not being as strong, they had more of an influence from the southwest and the east.

**Figure 93** shows correlation plots along with a temporal plot of particles matched to HDDV and LDV along with aethalometer data ( $\lambda = 880\text{nm}$ ). There is a stronger correlation between the aethalometer and the HDDV matched particles ( $R^2 = 0.77$ ) than



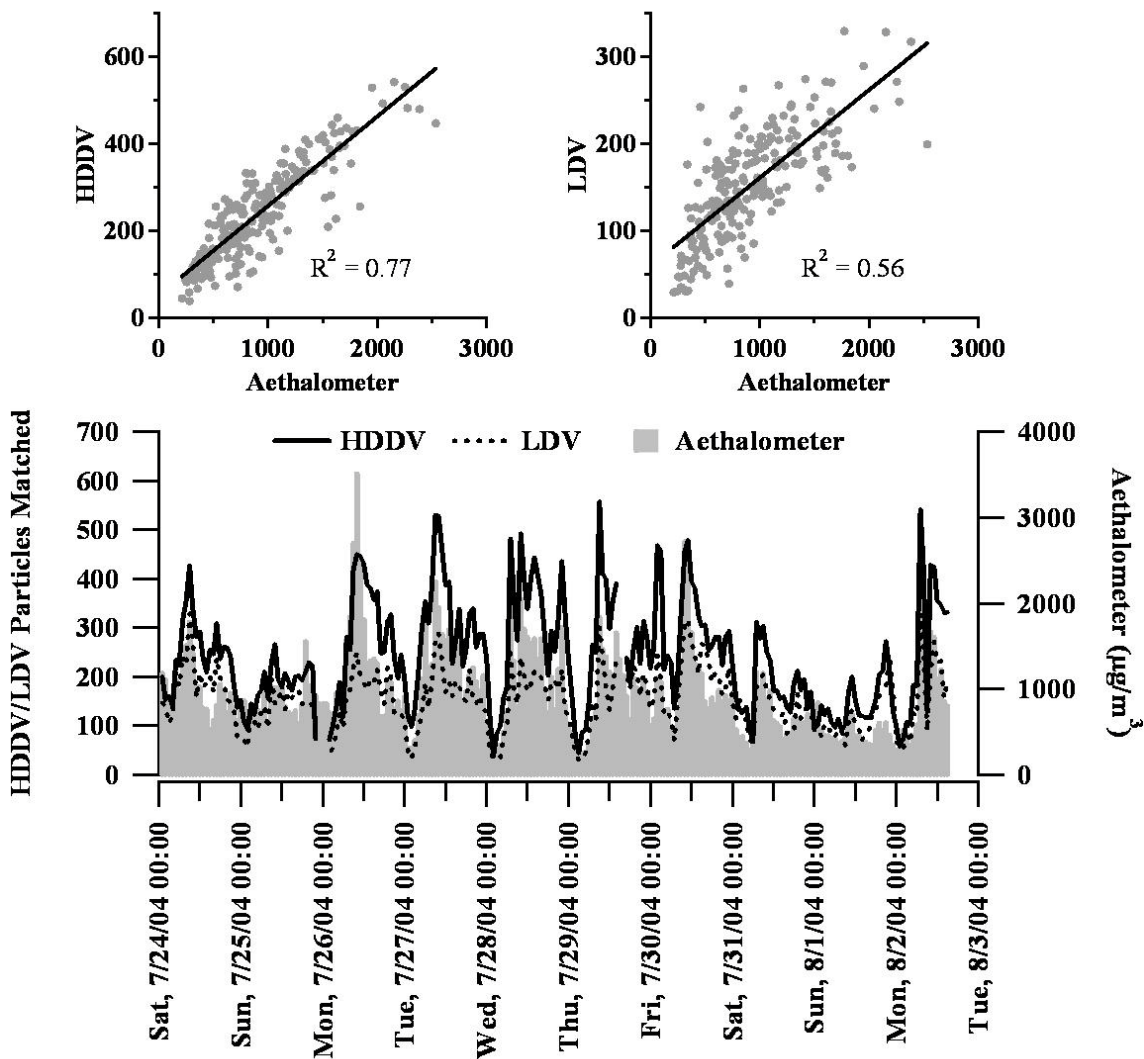


Figure 93: Time series of aethalometer data with HDDV/LDV apportioned particles. The  $R^2$  values for aethalometer to HDDV is 0.77, and 0.56 for the aethalometer to LDV.

with the LDV matched particles ( $R^2 = 0.56$ ). Aethalometers measure the absorptivity of particles in the UV to IR regions, and since HDDVs emit a larger number of elemental carbon than do LDVs, the trends of aethalometer data should reflect trends in HDDV exhaust particles. Based on the trends of the  $\text{NO}_x$  and aethalometer data with the ATOFMS data, the observed correlations provide support to the ART-2a apportionment approach used in this study. The results presented in this paper represent the first step in using mass spectral source signatures acquired in LDV and HDDV dynamometer source characterization studies for ambient source apportionment. As expected, a high percentage (83%) of the ultrafine and accumulation mode aerosols sampled near the freeway are attributed to vehicle exhaust emissions, with 32% and 51% being attributed to LDV and HDDV, respectively. Future studies using different algorithms, including Hierarchical clustering and Positive Matrix Factorization, will be performed and the

results will be compared to those obtained in this study. Also, comparisons will be made between single particle source apportionment results and standard organic tracer methods (433). Such comparisons will be necessary for determining the most appropriate method for performing source apportionment using single particle mass spectral data.

#### **iv. Acknowledgements**

The authors thank Dan Cayan and Alex Revchuk of the Scripps Institution of Oceanography (SIO) at UCSD for setting up the micro-meteorological stations and providing data for this study. We also thank UCSD and their facilities management for all their cooperation and help with setting up power to the sampling site, as well as the members from the Prather group who helped in transporting equipment to the site. This work was supported by the California Air Resources Board (CARB) (Contract 04-336).